CHEMICAL ENGINEERING TRANSACTIONS
VOL. 84, 2021
A publication of AIDIC
The Italian Association of Chemical Engineering
Online at www.cetjournal.it
Guest Editors: Paolo Ciambelli, Luca Di Palma

**ISBN** 978-88-95608-82-2; **ISSN** 2283-9216
DOI: 10.3303/CET2184032

# Alumina Based Electrode for Stable and Improved Supercapacitor Applications

Eleonora Ponticorvo[a*], Sergio Galvagno[b], Sabrina Portofino[b], Carmela Borriello[b], Loredana Tammaro[b], Pierpaolo Iovane[b], Gabriella Rametta[b], Maria Sarno[a]

[a]Department of Physics "E.R. Caianiello" and Centre NANO_MATES (Research Centre for Nanomaterials and Nanotechnology at the University of Salerno) University of Salerno, Via Giovanni Paolo II, 132 - 84084 Fisciano (SA), Italy
[b]Nanomaterials and Devices Laboratory (SSPT-PROMAS-NANO), ENEA, Italian National Agency for New Technologies, Energy and Sustainable Economic Development, Piazzale E. Fermi 1, 80055 Portici, NA, Italy
eponticorvo@unisa.it

This work describes the preparation of an $Al_2O_3$ electrode material for a performing and stable supercapacitor. The electrode was prepared by a DC thermal plasma plant installed at ENEA Research Centre of Portici. The structures and morphologies of samples were characterized by SEM, XRD, TG, and FT-IR. $Al_2O_3$ electrode electrochemical characteristics were performed in a sulphuric acid solution electrolyte. Cyclic Voltammetry (CV) technique was carried out. The results show that $Al_2O_3$ exhibits a good specific capacitance. Furthermore, after 10000 cycles, 98% of the initial capacitance was maintained.

## 1. Introduction

Energy availability and greenhouse gasses emission has become a problem related to the excessive consumption of traditional non-renewable sources (Wang et al., 2013). The development and the search for renewable green energy resources and, at the same time, better energy storing systems are urgently needed. Supercapacitors have attracted broad interest (Wang et al., 2007; Sarno et al., 2015) due to their high energy density, excellent cycle stability, high specific capacitance, and long life (Xia et al., 2012). According to the different energy storage mechanisms, supercapacitors can be classified into two main categories (Yang et al., 2012): the double-layer capacitors and the pseudocapacitors. In the double-layer capacitors (e.g., carbon materials), electrodes store energy by using the electrostatic capacitance of the interface double-layer. The pseudocapacitors, which has higher capacitance than double-layer capacitors, keep charge by a rapid and reversible redox reaction. As electrode materials, the metal oxides have attracted great interest due to their high capacitance characteristics in redox reactions. Numerous transition metal oxides and conducting polymers have been used. Aluminum oxide has many unique and attractive properties, such as large specific surface area, good thermal conductivity, inertness to most acids and alkalis, mechanical strength and stiffness, wear resistance, high adsorption capacity, and thermal stability. Moreover, $Al_2O_3$ is also non-toxic, highly abrasive, and inexpensive (Mallakpour and Khadem, 2015; Mirjalili et al., 2011; Gunday et al., 2019). These properties make $Al_2O_3$ suitable for various applications such as catalysts, sensors, and supercapacitors. In particular, the supercapacitor performance of a ternary electrode, constituted by γ-$Al_2O_3$ nanoparticles, polyindole, and reduced graphene oxide, was reported (Azizi et al., 2020). The beneficial effect of $Al_2O_3$ in improving and enhancing the conductive polymer electrochemical stability and capacitance, thanks to catalyzing redox reactions ability, was demonstrated. However, to the best of our knowledge, the electrochemical properties of an electrode constituted by the only alumina with high purity and morphological uniformity have never been reported. In order to form a stable, cheap, and performing electrode, here we report the use of $Al_2O_3$ powders, prepared by thermal plasma technique, for supercapacitor applications. Among high purity and fine powders synthesis procedures, the vapor phase reactions that avoid complex and expensive preparative steps, usually required in chemical processes, i.e., precipitation and purification, are particularly helpful for the production of deagglomerated particles with a narrow size distribution (Iovane et al., 2019; Hong and Yan, 2018). Scanning Electron Microscopy (SEM), thermogravimetric analysis (TG), Fourier

Paper Received: 30 July 2020; Revised: 5 January 2021; Accepted: 18 February 2021
Please cite this article as: Ponticorvo E., Galvagno S., Portofino S., Borriello C., Tammaro L., Iovane P., Rametta G., Sarno M., 2021, Alumina Based Electrode for Stable and Improved Supercapacitor Applications, Chemical Engineering Transactions, 84, 187-192 DOI:10.3303/CET2184032

Transform Infrared Spectroscopy (FTIR), and X-ray diffraction (XRD) were used for characterization. The electrochemical performances of the electrode were investigated by cyclic voltammetry tests. The results of CV measurements proved that this kind of supercapacitor has good electrochemical capacitance performance within a wide potential range and improved electrochemical stability.

## 2. Experimental

### 2.1 Sample preparation

Aluminum oxide powder (particle size 0,5-1mm) was milled by Retsch PM100 (planetary ball mill) using a 500 ml steel jar and 1 cm diameter balls and 1/3 balls, 1/3 empty and 1/3 powder ratio. The powder was sieved in 40-63 μm range by Retsch AS basic 200 after milling and drying in an oven at 105 °C. This powder was treated by a DC thermal plasma plant installed at ENEA Research Centre of Portici (Iovane et al., 2019). The system comprises a powder feeder system, a DC non-transferred plasma torch, a power supply (80 kW), a cyclone/bag filter, and a dry scroll pump for vacuum. The plasma operates under a light vacuum (up to 20 kPa). The torch consists of a water-cooled tungsten cathode and a copper anode nozzle. It is fitted in the upper part of a jacketed-cylindrical stainless steel reactor of 13 cm inner diameter, and 185 cm length cooled with circulating cold water. The reactor is equipped with a collection tank, where the produced powders are collected along with the unreacted materials. At the top of the reactor, one nozzle feeds the powder directly into plasma fame (internal feed). The test has been conducted using argon (Ar) as the main gas (about 40 slpm) to light the plasma and helium (He) (about 10 slpm) as secondary gases to improve the flame conditions. Other experimental conditions were fixed: the plasma torch power at 20 kW, the gas flow rate (Ar) at 0,5 slpm, the powder feeding rate at 2 g/min, the pressure of the reaction chamber 87 kPa. The powder produced was sieved under 25μm by Retsch AS basic 200.

### 2.2 Characterization methods

The combined use of different techniques obtained the sample characterization. Scanning electron microscopy (SEM) images were received using a LEO 1530 equipped with a filament of tungsten at 4 kV and working under high vacuum conditions, equipped with an energy dispersive X-ray (EDX) probe. A Bruker D8 X-ray diffractometer with a monochromatic CuK$\alpha$ radiation was used for measurements of powder diffraction profiles. The thermal behavior of the samples was investigated using TG and derivative thermogravimetric (DTG) analysis (Mettler Toledo TGA, Model) between 25 and 1000 °C under airflow (60 mL $min^{-1}$) with a heating rate of 10 °C $min^{-1}$. FTIR was recorded on the Fourier transform infrared spectrometer BRUKER VERTEX-70, (Bruker Corporation). The surface area was obtained by $N_2$ adsorption-desorption at 77 K (Kelvin 1042 V3.12, COSTECH Instruments). Electrochemical tests to evaluate the synthesized samples' capacitance performances, in particular cyclic voltammetry (CV) tests, were carried out by means of an Autolab PGSTAT302N potentiostat. In detail, cyclic voltammetry measurements were run at different scan rates (10, 20, and 50 mV/s) in the potential range 0 ÷ 0.8 V and in a 0.5 M $H_2SO_4$ electrolyte solution. Starting from the CV, the Eq (1) was used in order to evaluate the specific capacitance of the samples:

$$C_{SP} = \frac{\int I \cdot dV}{\Delta V \cdot v} \quad (1)$$

ΔV is the potential range chosen, I is the current density, V is the potential, v is the CV scan rate.
Before performing the tests, 4 mg of synthesized material were dispersed into 80 μl of a 5 wt% Nafion solution, 200 μl of ethanol, and 800 μL of water. The resulting mixture consists of a homogeneous suspension which, after being sonicated for 30 mins and then air-dried, was partially deposited dropwise onto a DRP-110 Screen Printed Electrode (SPE). SPE consisted of a carbon working electrode, a platinum counter electrode, and a silver reference electrode and was preferred over commonly used carbon electrodes thanks to their excellent characteristics (Rowley-Neale et al., 2015; Sarno and Ponticorvo, 2018; Sarno et al., 2019).

## 3. Results and discussion

### 3.1 Chemical and morphological characterization

As shown in Figure 1, the XRD pattern of the prepared sample consists of α-$Al_2O_3$ phase, corresponding to (012), (104), (110), (113), (024), (116), (211), (018), (214), (300) and (119) planes at 24.84°, 34.65°, 37.27°, 43.90°, 52.01°, 57.10°, 58.81°, 60.83°, 66.04°, 67.84°, and 76.90°, according to ICDD (The International Centre for Diffraction Data) JCPDS No. 00-010-0173. The powders morphology was evaluated by SEM. The plasma synthesis takes place in the gaseous phase, where new particles are nucleated in the tail of the fame. Applying fast quenching, the particles tend to form a uniform spherical shape in order to minimize their specific surface areas and surface energy (Iovane et al., 2019), which enable effective electrolyte access into the

electrode and is favorable for better supercapacitor performance (Xiao et al., 2017). SEM characterization (Figure 2) of the sample shows good results in terms of spherical shape, where the powder displays aggregate with roundness (RN) higher than 80%.

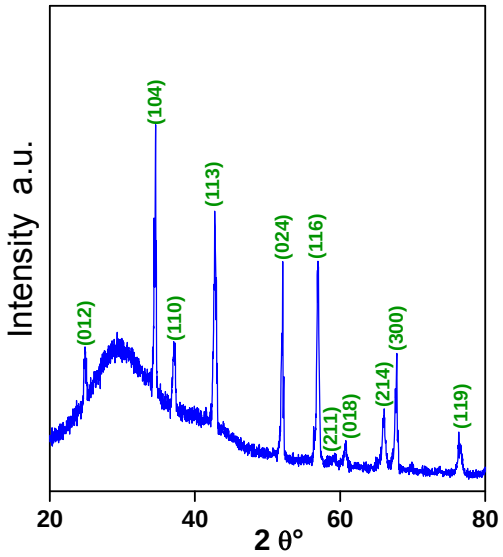


*Figure 1: XRD patterns of $Al_2O_3$ powder*

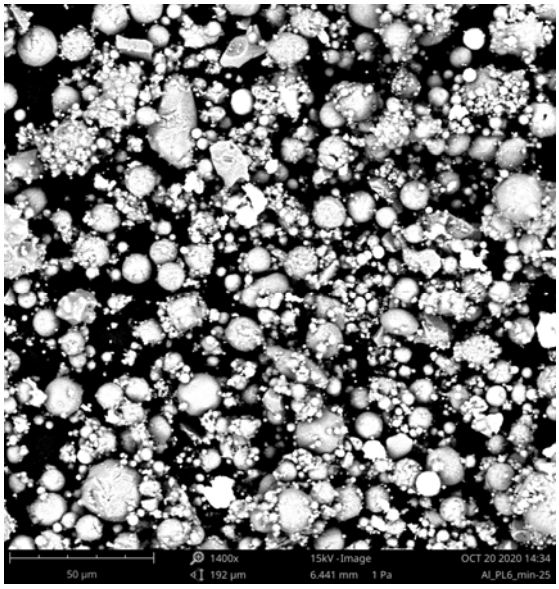


*Figure 2: SEM image of $Al_2O_3$ powder*

Thermogravimetric analysis (TG) thermograph (Figure 3) with soft loss and without sharp peaks proofs single-phase and no impurity in the sample. As shown in Figure 3, the weight loss (~ 1 %) occurs at temperatures lower than 400 ºC due to the evaporation of volatile components, such as water residues, including adsorbed water, free water, crystal water.

The FTIR spectra of the α-$Al_2O_3$ samples are shown in Figure 4. The intense bands between 500 and 1000 $cm^{-1}$ are related to the vibrational frequencies of O–Al–O bonds (Aman et al., 2013). This band was divided into two bands, which are the most characteristic FTIR feature.

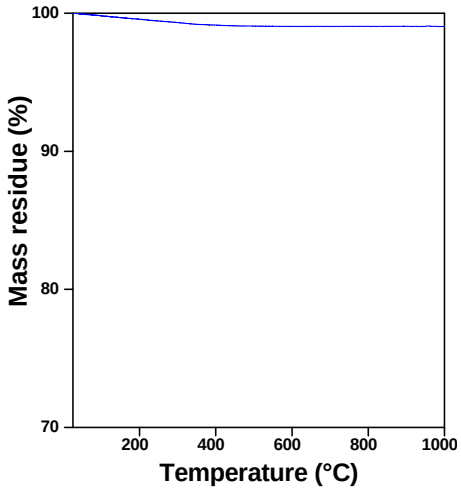


*Figure 3: TG profile of $Al_2O_3$ powder*

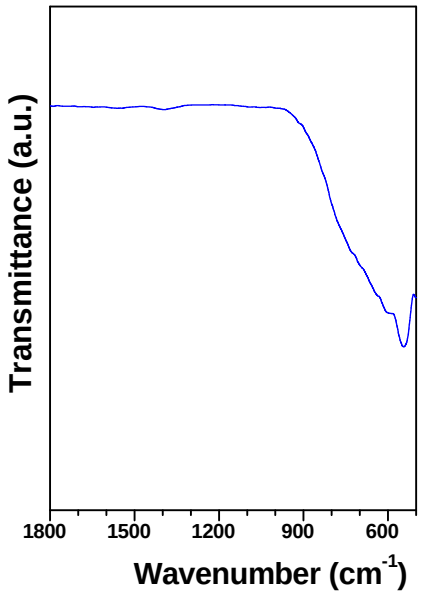


*Figure 4: FTIR spectrum of $Al_2O_3$ powder*

### 3.2 Electrochemical characterization

CV curves of the prepared sample at different scan rates (10, 20, and 50 mV/s) were reported in Figure 5. From the figure, we can see that the $Al_2O_3$ electrode show quasi-rectangular current–voltage response curves. No detectable redox peaks can be found in the chosen potential window, which indicates a nearly ideal capacitive behavior (Wang et al., 2015; Du et al., 2009; Yoo et al., 2011; Zhu et al., 2010; Sarno et al., 2016; Karandikar et al., 2012; Nishihara et al., 2012; Sarno et al., 2019).

A capacitance of ~ 10 F/g was obtained. Moreover, long-term cycling tests were carried out in 0.5 M $H_2SO_4$ over 10000 cycles at 20 mV/s, proving that 98 % of the initial capacitance was retained (Figure 6). However, the presence of highly conductive material to promote charge transport and accumulation is the most required feature for supercapacitors electrodes (Pandolfo et al., 2006). Therefore, the obtained encouraging results suggest the possibility to achieve even higher capacitances further by adding more conductive double-layer supercapacitive materials, such as graphene. The loading of graphene will be the subject of future dedicated works.

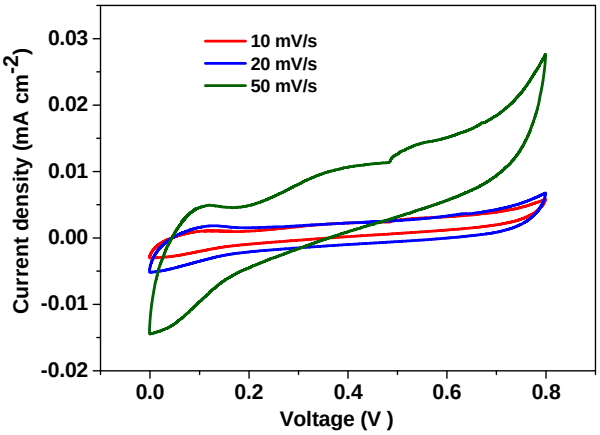


*Figure 5: Cyclic voltammograms measured at different scan rates in a 0.5 M $H_2SO_4$ solution.*

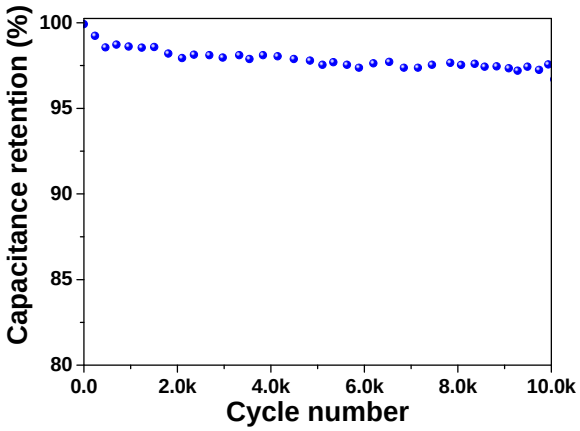


*Figure 6: Capacitance retention as a function of cycle number.*

## 4. Conclusions

In summary, an efficient procedure was adopted in order to prepare $Al_2O_3$ powder by a DC thermal plasma plant installed at ENEA Research Centre of Portici. SEM, FT-IR, XRD, and TG analyses confirmed the formation of the above-mentioned sample. Cyclic voltammograms, run at different scan rates in a 0.5 M $H_2SO_4$ solution, revealed that the $Al_2O_3$ powder exhibits quasi-rectangular current–voltage response curves without any detectable redox peaks in the analyzed potential window, which suggests a nearly ideal capacitive behavior thanks to the accessibility and wettability of the electrode for ion adsorption. Moreover, the synthesized $Al_2O_3$ powder exhibited very high capacitance retention, showing high stability as well as promising capacitive performance as robust electrode material.

### Acknowledgments

This research was supported by MiSE-ENEA bilateral program agreement "Research on Electric System" – Project 1.3 "Materiali di frontiera per usi energetici-Frontier materials for energy uses" (ADP MiSE-ENEA Piano Triennale di Realizzazione 2019-2021) – ENEA-NANO_MATES cooperating agreement “Materiali e componenti per additive manufacturing, con impatto sul sistema elettrico - Materials and components for additive manufacturing, with an impact on the electrical system” .

### References

Aman Y., Rossignol C., Garnier V., Djurado E., 2013, Low temperature synthesis of ultrafine non vermicular α-alumina from aerosol decomposition of aluminum nitrates salts, Journal of the European Ceramic Society, 33, 1917-1928.

Azizi E., Arjomandi J., Salimi A., Lee J.Y., 2020, Fabrication of an asymmetric supercapacitor based on reduced graphene oxide/polyindole/γ - $Al_2O_3$ ternary nanocomposite with high-performance capacitive behavior Polymer, 195, 122429.

Du X., Wang C., Chen M., Jiao Y., Wang J., 2009, Electrochemical performances of nanoparticle $Fe_3O_4$/active carbon supercapacitor using KOH electrolyte solution, Journal of Physical Chemistry C, 113, 2643–2646.

Gunday S.T., Cevik E., Yusuf A., Bozkurt A., 2019, Fabrication of $Al_2O_3$/IL-Based Nanocomposite Polymer Electrolytes for Supercapacitor Application, ChemistrySelect, 4, 5880– 5887.

Hong F.C.N., Yan C.J., 2018, Synthesis and characterization of silicon oxide nanoparticles using an atmospheric DC plasma torch, Advanced Powder Technology, 29, 220–229.

Iovane P., Borriello C., Portofno S., De Girolamo Del Mauro A., Magnani G., Minarini C., Galvagno S., 2019, Thermal Plasma Synthesis of Zirconia Powder and Preparation of Premixed Ca□Doped Zirconia, Plasma Chemistry and Plasma Processing, 39, 1397-1411.

Karandikar P.B., Talange D.B., Mhaskar U.P., Bansal R., 2012, Development, modeling and characterization of aqueous metal oxide based supercapacitor, Energy, 40, 131-138.

Mallakpour S., Khadem E., 2015, Recent development in the synthesis of polymer nanocomposites based on nano-alumina, Progress in Polymer Science, 51, 74-93.

Mirjalili F., Hasmaliza M., Chuah L., 2011, Preparation of nano scale α-$Al_2O_3$ powder by the sol-gel method, Journal Ceramics-Silikáty, 55, 378–383.

Nishihara H., Kyotani T., 2012, Templated nanocarbons for energy storage, Advanced Materials, 24, 4473-4498.

Pandolfo A.G., Hollenkamp A.F., 2006, Carbon properties and their role in supercapacitors, Journal of Power Sources, 157, 11-27.

Rowley-Neale S.J., Brownson D.A.C., Smith G.C., Sawtell D.A., Kelly P.J., Banks C.E., 2015, 2D nanosheet molybdenum disulphide ($MoS_2$) modified electrodes explored towards the hydrogen evolution reaction, Nanoscale, 7, 18152–18168.

Sarno M., Baldino L., Scudieri C., Cardea S., Ciambelli P., Reverchon E., 2016, Supercritical $CO_2$ processing to improve the electrochemical properties of graphene oxide, The Journal Of Supercritical Fluids, 118 119–127.

Sarno M., Cirillo C., Ponticorvo E., Ciambelli P., 2015, Sythesis and Characterization of FLG/$Fe_3O_4$ Nanohybrid Supercapacitor, Chemical Engineering Transactions, 43, 943-948.

Sarno M., Ponticorvo E., 2018, Continuous flow HER and MOR evaluation of a new Pt/Pd/Co nano electrocatalyst, Applied Surface Science, 459, 105-113.

Sarno M., Ponticorvo E., Scarpa D., 2019, Ru and Os based new electrode for electrochemical flow supercapacitors, Chemical Engineering Journal, 377, 120050.

Wang S., Wei T., Qi Z., 2007, Supercapacitor Energy Storage Technology and its Application in Renewable Energy Power Generation System, Proceedings of ISES World Congress, Vol.I-Vol.V, 2805-2809.

Wang Z., Liu C.J., 2015, Preparation and application of iron oxide/graphene based composites for electrochemical energy storage and energy conversion devices: current status and perspective, Nano Energy, 11, 277–293.

Wang Z., Ma C., Wang H., Liu Z., Hao Z., 2013, Facilely synthesized $Fe_2O_3$–graphene nanocomposite as novel electrode materials for supercapacitors with high performance, Journal of Alloys and Compounds, 552, 486–491.

Xia X., Hao Q., Lei W., Wang W., Sun D., Wang X., 2012, Nanostructured ternary composites of graphene/$Fe_2O_3$/polyaniline for high-performance supercapacitors, Journal of Materials Chemistry, 22, 16844–16850.

Xiao X., Han B., Chen G., Wang L., Wang Y., 2017, Preparation and electrochemical performances of carbon sphere@ZnO core-shell nanocomposites for supercapacitor applications, Scientific Reports, 7, 40167.

Yang W., Gao Z., Wang J., Wang B., Liu Q., Li Z., Mann T., Yang P., Zhang M., Liu L., 2012, Synthesis of reduced graphene nanosheet/urchin-like manganese dioxide composite and high performance as supercapacitor electrode, Electrochimica Acta, 69, 112–119.

Yoo J.J., Balakrishnan K., Huang J., Meunier V., Sumpter B.G., Srivastava A., Conway M., Mohana Reddy A.L., Yu J., Vajtai R., 2011, Ultrathin Planar Graphene Supercapacitors, Nano Letters, 11, 1423−1427.

Zhu Y., Stoller M.D., Cai W., Velamakanni A., Piner R.D., Chen D., Ruoff R.S., 2010, Exfoliation of Graphite Oxide in Propylene Carbonate and Thermal Reduction of the Resulting Graphene Oxide Platelets, ACS Nano, 4, 1227−1233.